Effects of Bruising of 'Pink Lady' Apple Under Impact Loading in Drop Test on Firmness, Colour and Gas Exchange of Fruit During Long Term Storage

H. Kursat CELIK[1,*], Hayri USTUN[2] , Mustafa ERKAN[2], Allan E.W. RENNIE[3], Ibrahim AKINCI[1]

[1,] Dept. of Agricultural Machinery and Technology Engineering, Fac. of Agriculture, Akdeniz University, Antalya, Turkey*
[2] Dept. of Horticulture, Fac. of Agriculture, Akdeniz University, Antalya, Turkey
[3]Engineering Dept., Lancaster University, Lancaster, United Kingdom

Corresponding author	*: Dr H. Kursat CELIK*
e-mail	*: hkcelik@akdeniz.edu.tr*
Tel	*: +90 242 310 65 70*
Fax	*: +90 242 310 24 79*
Address	*: Dept. of Agricultural Machinery and Technology Engineering, Akdeniz University, 07070, Antalya, Turkey*

ABSTRACT

The bruising phenomenon of apple fruit under impact loading is still a very important problem to be solved in order to design optimal harvest and processing systems and for ensuring the quality of the fruit during long-term periods of storage. This study focused on deformation simulation of apples (cv. 'Pink Lady') under dynamic impact loading during drop tests in order to describe time-dependent bruising occurrence and the bruising effect on the postharvest fruit quality during long-term storage. In the study, analytical, experimental methods and finite element analysis based explicit dynamics simulation techniques were employed. Three drop heights (250 mm, 500 mm and 750 mm) and three impact materials (structural steel, high-density polyethylene and wood) and single fruit orientation (transverse) for the drop tests were considered. Experimental drop test, physical and chromatographic analyses at the time of harvest (first testing day) and during storage periods of 30, 120 and 210 days were realised. Physical and chromatographic analyses revealed that damaged apples lost a greater amount of weight when considering the increase in drop height. Furthermore, bruised surfaces of apples lost their luminosity just after the drop test. Ethylene production and respiration rates rapidly increased just after the fruit bruising and this increase was correlated with the drop height. Additionally, material tests revealed the yield stress point of the apple as 0.385 MPa and the simulation results provided useful visuals and numerical data related to the time-dependent bruising phenomenon. The validation study on the experimental and simulation setup revealed that bruising surface area is a more accurate measurement than bruise volume when evaluating bruising on the fruit flesh through a numerical method-based simulation study (average relative difference: 5.5%).

KEYWORDS: Pink Lady, Apple, Bruising, Quality, Drop Test, Finite Element Analysis

[1]H. Kursat CELİK, PhD, Assoc. Prof	*hkcelik@akdeniz.edu.tr*	*ORCID: 0000-0001-8154-6993*
[2]Hayri USTUN, PhD Candidate	*hayriustun07@gmail.com*	*ORCID: 0000-0003-1876-0481*
[2]Mustafa ERKAN, PhD, Prof.	*erkan@akdeniz.edu.tr*	*ORCID: 0000-0001-9729-9392*
[3]Allan E.W. RENNIE, PhD, Prof.	*a.rennie@lancaster.ac.uk*	*ORCID: 0000-0003-4568-316X*
[1]Ibrahim AKINCI, PhD, Prof.	*iakinci@akdeniz.edu.tr*	*ORCID: 0000-0002-0057-0930*

Word Counts	*: Approx. 7190 (Excluding References and Figure/Table Captions)*
Number of Figures	*: 9*
Number of Tables	*: 4*

1. INTRODUCTION

Apple (*Malus* x *domestica* Borkh.) is one of the most produced and consumed fruit in the world. The global production of apples is 87.24 million tons (MT), where China ranked 1st (42.43 MT), followed by the USA (5 MT), Turkey (3.62 MT) and Poland (3.08 MT) (FAOSTAT, 2019). Apple is a rich source of vitamins, phenolics, organic acids, antioxidants and fibres for the human diet (Mditshwa et al., 2018; Musacchi and Serra, 2018). Apples experience laborious stages starting from the tree in an orchard through to final consumption. During these stages, apples undergo many processes including harvesting, packing, sorting, storage, transport and marketing (Lewis et al., 2008). Mechanical damage is the main problem during these processes and has the potential to significantly reduce the quality of the product, which results in a lower market value. Therefore, quality loss due to mechanical damage during postharvest operations has become a major problem in the fresh produce industry (Fadiji et al., 2016). During these processes, fruit may be bruised through physical effects such as fingerprints, dropping, squeezing, packing pressure, etc. Bruising that mostly occurs during the harvesting, sorting, packing and marketing stages, is the most common type of mechanical injury for almost all fresh fruit and vegetables (Knee, 2001; Van Zeebroeck et al., 2007). In this context, specific to apple fruit, the literature highlights that most laboratory studies have involved impact energies above 0.1 J producing clear visible bruising (Van Zeebroeck et al., 2007). Therefore, when apples drop from heights, which produce impact energy above 0.1 J, on to different surfaces such as steel, plastic or wood, the damage mainly initiates on the fruit surface and the internal composition of the fruit becomes vulnerable to decay over time. Furthermore, the damage in almost all produce as well as apples may lead to an increase in ethylene production, micro and macro skin cracks, peel crushing and quality loss.

In this context, understanding the fruit deformation behaviour under dynamic impact/drop loading has become a very important issue to be solved in order to design optimal agricultural/food product processing and packaging systems found in related industries and the longer-term storage issues of the products. During the initial design phases of the machinery systems, some related features (constituting design parameters), such as engineering properties, deformation behaviour and bruise susceptibility of the products under dynamic deformation cases, should be clearly described; however, this may become very complicated (Celik, 2017). Bruising issues were discussed in the work of Opara and Pathare (2014) related to measurement and analysis of the mechanical bruising damage of fresh horticultural produce. The review indicated that there is no agreed common criterion which can assess the amount of bruise susceptibility, however, in addition to absorbed energy calculation, two physical measurements, which are the bruise area and the bruise volume, are the most common for mechanical damage. Bruise susceptibility can be calculated as the amount of damage per unit of absorbed impact/compression energy (Brusewitz and Bartsch, 1989; Celik, 2017; Garcia et al., 1988; Holt and Schoorl, 1977; Opara and Pathare, 2014; Pang et al., 1996). In addition to this, although, Opara and Pathare (2014) highlights that the bruise volume is the most commonly reported measure of the amount of bruise damage, Pang et al. (1996) claimed that the bruise surface area was a better parameter than the bruise volume for assessing the product damage.

The literature on this issue reveals that many researchers have utilised various destructive and non-destructive experimental methods to determine the bruise susceptibility of fruit under dynamic impact loading. The pendulum test was found to be a prevalent destructive method utilised by researchers (Abedi and Ahmadi, 2013; Eissa et al., 2012; Komarnicki et al., 2016). Non-destructive defect detection of apples through image processing technologies was also commonly studied (Lu and Lu, 2017). However, these experimental methods did not illustrate and describe the internal bruise phenomenon at the dynamic deformation cases such as impact loading during drop of a fruit, since the bruise is a type of subcutaneous tissue failure without rupture of the skin of such products (Mohsenin, 1986). As such, numerical method-based engineering analysis and simulation techniques such as Finite Element Analysis (FEA) may offer a promising avenue for solving such complicated loading conditions of the fruit, as this simulation technique has been found to be useful in the research field of the deformation analysis of agricultural products (Cardenas-Weber et al., 1991; Celik et al., 2011; Kabas et al., 2008).

The objectives of this research are to describe the time dependant bruising phenomenon of a 'Pink Lady' apple under dynamic impact loading during drop test by means of finite element method (FEM) based explicit dynamics simulation, and to assess the postharvest fruit quality of damaged apples during long-term storage through physical and chromatographic analyses.

2. MATERIAL AND METHODS

2.1. Application Algorithm

In this research, an application algorithm which can be integrated to bruising analysis studies for agricultural products was developed and a specific study on bruising analysis of a 'Pink Lady' apple was realised. The algorithm was constructed based on physical and chromatographic analyses, experimental material testing and computer aided engineering simulation techniques. The core application sequence of the developed algorithm is illustrated in Figure 1.

(**Fig. 1.** Application algorithm for bruising and quality investigation of 'Pink Lady' apple)

2.2. Fruit Material

'Pink Lady' apples were harvested at the physiological maturity stage by using a starch-iodine test in the orchard at Elmalı, Antalya, Turkey (36° 37' 13.7" N 29° 52' 37.3" E). Fruit characteristics at harvest were determined as having fruit firmness 84.44 N, soluble solid contents 16.33 % and titratable acidity 0.77 g malic acid 100^{-1} mL. After harvesting, the apples for analyses were selected based on size uniformity and that they had no visual defects.

2.3. Experimental Drop Test

In the drop test experiments, undamaged whole apple specimens were allowed to free fall impact onto a flat platform from predefined impact heights under standard earth gravity. A portable drop test apparatus was designed for the experiment. Three drop heights (250 mm, 500 mm and 750 mm), three flat form materials for the fruit impact which are referred to as impact surfaces (structural steel, high-density polyethylene (HDPE), and wood (spruce) materials) and single impact orientations (transverse) were set-up for the experiments. During the experiments, the specimens were intercepted after the first impact rebound and not allowed to make second contact with the impact surface, in order to investigate single drop bruising. Ten specimens for each drop test scenario were utilised. In addition to first day investigation (Day 0) of the samples, they were left on the lab bench at 20°C for 24 h after the drop test, the remainder of the specimens were carefully moved to a cold storage unit where they were kept at 0 °C for additional investigation periods. After each of the storage periods (Day-0, Day-30, Day-120 and Day-210), in addition to physical and chromatographic analyses, measurements of the bruise areas and the bruise volumes of the tested apple specimens were undertaken. In this study, three parameters (i.e. bruise area, bruise volume and absorbed energy at impact) for assessing damage simulation of the apples were considered. In fact, determination of bruise volume of an organic material exposed to a mechanical impact is a difficult phenomenon to observe through physical experiments against bruise area measurement. Further research on this topic reported that bruise volume estimation methods in the scientific literature induce errors in prediction of the actual volume and there is no single method established for the estimation of bruise volume (Bollen et al., 1999). The portable drop test apparatus and testing scenario utilised in this study are illustrated in Figure 2. Related to bruising calculations, the empirical expressions for the bruise measurements utilised in this study are given in Equations 1-6 (Mohsenin, 1986; Opara and Pathare, 2014; Pang et al., 1996). The abbreviations used in the equations and related dimensions are listed in Table 1.

(**Fig. 2**. The portable drop test apparatus, testing scenario (a) and the dimensions used in bruising assessment (b))

$$E_i = m \cdot g \cdot h \quad (1)$$

$$E_A = m \cdot g \cdot (h_d - h_r) \quad (2)$$

$$A_b = \frac{\pi}{4}(W_{b1} \cdot W_{b1}) \quad (3)$$

$$V_b = \frac{\pi \cdot d_b}{24}(3W_{b1} \cdot W_{b1} + 4{d_b}^2) \quad (4)$$

$$S_{bA} = \frac{A_b}{E_A} \qquad (Area\, based) \quad (5)$$

$$S_{bV} = \frac{V_b}{E_A} \qquad (Volume\ based) \quad (6)$$

(**Table 1.** List of the abbreviations used in the equations and related dimensions)

2.4. Storage and Sampling Details

Following the experimental drop test, the fruit specimens were stored at 0 ºC and 85-90 % relative humidity (RH) for up to 210 days at Postharvest Physiology Laboratory of Akdeniz University Antalya, Turkey. Fruit samples were collected from the storage at 30, 120, and 210 day intervals in order to conduct visual observations, bruise measurements, analyse and final evaluation.

2.5. Physical and Chromatographic Analyses

The weight loss of the fruit was measured with digital scales with 0.01 precision (in grammes), calculated on an initial mass basis and then finally it was expressed as a percentage. The fruit flesh firmness was measured on three areas of the surface using a fruit firmness penetrometer (EFFEGI-FT 327, FACCHINI srl, Italy) with an 11.1 mm probe and expressed as Newton (N). The total soluble solids content was measured in the apple juice with a digital refractometer (Hanna HI96801, Hanna Instruments, USA) and then expressed as a percentage. Titratable acidity was performed with 2 mL juice + 38 mL distilled water by titrating with 0.1 N NaOH up the 8.1 pH using a pH meter and the results were expressed in g malic acid 100^{-1} mL juice. Changes in skin colour were measured as Lightness (L*), Chroma (C*) and Hue angle (hº) with the aid of a Minolta Chroma Meter (Model CR 400, Minolta, Tokyo, Japan). The measurements were performed on damaged and non-damaged surfaces of the fruit and the mean value was computed for each group. The respiration rate of the fruit was determined with gas chromatography (GC) (Thermo Finnigan Trace GC Ultra, Thermo Electron S.p.A. Strada Rivoltana 20900 Radano, Milan, Italy). For respiration rate measurements, eight apples (approx. 1.5 kg) from each replication were kept in 5 L gas-tight jars for 1 h at 20 ºC. For that purpose, a 1 mL gas sample was taken from the headspace of jars and injected into GC equipped with a thermal conductivity detector. The results were calculated as mL CO_2 kg^{-1} h^{-1}. Chromatographic conditions of respiration rate measurement were as follows: 80/100 porapak n column, 65 ºC oven temperature, 100 ºC detector temperature, 100 ºC injection temperature, 10 mL min^{-1} helium flow, 20 mL min^{-1} hydrogen flow, 30 mL min^{-1} nitrogen flow and 4 minutes analysis time. The ethylene production of the fruit was determined with GC. For ethylene production measurements, eight apples (approx. 1.5 kg) from each replication were kept in 5 L gas-tight jars for 1 h at 20 ºC. Then a 1 mL gas sample was taken from the headspace of the jars and injected into GC equipped with a flame ionization detector. The ethylene production was calculated as µL C_2H_4 kg^{-1} h^{-1}. Chromatographic conditions of ethylene production measurement were as follows: 80/100 alumina f^{-1} column, 90 ºC oven temperature, 170 ºC detector temperature, 150 ºC injection temperature, 25 mL min^{-1} helium flow, 35 mL min^{-1} hydrogen flow, 350 mL min^{-1} nitrogen flow and 2 min analysis time. For ethylene and respiration, measurements were carried out on the fruit from cold storage on days 30, 120 and 210. The same measurements were also carried out just after the damage occurrence on the fruit at 20 ºC.

2.6. Statistical Analyses Related to Physical and Chromatographic Analyses Results

The statistical analyses were conducted according to completely randomised design with three replications and each replication containing 10 apples. The parameters of treatment, storage duration and treatment x storage duration interaction were examined through a general linear model. All statistical analyses were performed through XLSTAT (version 2016.02.28451, Addinsoft, France). Least Significant Difference (LSD) test was utilised for the comparison of means ($P \leq 0.05$).

2.7. Finite Element Analysis (FEA)

2.7.1. Computer Aided Design (CAD) Modelling of the Apple Specimen

An apple specimen was digitised for the drop test simulation study. The Specimen was selected randomly from non-damaged whole apple specimens. A reverse engineering approach was utilised to create the apples 3-Dimensional (3D) computer aided design (CAD) model in order to simulate an accurate drop test with a realistic apple geometry. A NextEngine-2020i 3D desktop laser scanner was employed in the digitisation of the apple and then the point cloud data obtained from the scanner was processed using Scan-StudioHD and SolidWorks (Dassault System, USA) 3D parametric design software. Some dimensional properties of the digitised apple specimen were measured on the CAD model. Dimensional features of the apple specimen are given in Table 2, respectively.

(**Table 2.** Dimensional features of the apple)

2.7.2. Determination of Material Properties and Physical Measurements

Material properties of the apple specimens such as elastic modulus, Poisson's ratio, bio-yield stress point, density and moisture content were experimentally determined through mechanical tests and physical measurements. The whole apple specimens used in this material testing procedure were previously kept in a cold storage unit at 0 ºC and then all specimens were moved to the test laboratory. The physical investigations were realised on randomly selected apple specimens at an ambient room temperature of 20 ºC. Related measurements and mechanical tests of the experimental procedure were conducted at the Biological Material Test Laboratory of the Department of Agricultural Machinery and Technology Engineering, Akdeniz University (Antalya, Turkey). Parallel plate compression tests were utilised for the cylindrical specimens (specimen dimensions: Ø20 x 25 mm). The cylindrical specimens were extracted from the whole apple (apple flesh). A universal compression test device was utilised for the compression tests. Loading capacity of the test device was 2000 N and the test data were collected by a computer aided data acquisition system connected to the test device. The compression test procedure for food/agricultural materials was described in detail in accordance with the standard ASAE S368.4 DEC2000 (R2017) (ASABE Standard, 2017). The ASABE Standard highlights that for specimens such as apples, the bio-yield point is best observed at speeds below 10 mm min^{-1}. Therefore, a compression plate travelling speed of 5 mm min^{-1} was set up in all tests. Each of the compression tests were carried out for 10 specimens. The data sampling rate was 10 Hz during the tests. Data of the compressive force against specimen deformation were simultaneously read during the test and then these data were processed. Finally, the test data were graphically represented. The cylindrical specimens were tested for the same moisture content (MC) (average MC: 82.79 ± 2.15 %, wet base, 10 specimens). A Nuve-FN 032/055/120 dry air steriliser (Nuve, Turkey) was utilised for the drying operation. The average moisture content of the specimens was calculated after the drying operation (24 hours at 105 ºC) (Sitkei, 1987). Average density of the apple flesh was calculated by measuring the volume and mass of the cylindrical test specimens extracted from the whole apple. Finally, material properties to be assigned in the FEA scenarios were experimentally described using a bi-linear isotropic homogeneous elastoplastic material model (Supplementary file-1).

2.7.3. Drop Test Simulation

A nonlinear FEM-based explicit dynamics simulation approach was utilised for the drop test simulation of the apple bruising. Nine simulation scenarios were set up in total. These drop test scenarios were simulated for various drop height and impact surface combinations. An explicit dynamics module of the ANSYS Workbench commercial FEM code (Ansys Inc., USA) was utilised to simulate the dropping scenarios. The apple was modelled as a homogeneous flesh structure. The frictional contact definitions between the apple and the surfaces, standard earth gravity of 9.8066 m s^{-2}, and an idealised material model (bi-linear isotropic homogeneous elastoplastic material model) for the apple model was defined. An identical curvature based and local sizing meshing strategy was applied in the creation of the finite element models used in the simulations. A total of 171097 elements and 41102 nodes were obtained in the finite element model. The mesh quality of the finite element model was verified through a skewness metric. Skewness is one of the primary quality measures for a mesh structure, which determines how close to ideal a face or cell is. According to the definition of skewness, a value of 0 indicates an equilateral cell (best) and a value of 1 indicates a completely degenerate cell (worst) (ANSYS Product Doc., 2019a). The average skewness metric value obtained was 0.207 which indicated an excellent cell quality for the finite element model. The simulation solve times were assigned under consideration of the first impact moment, bruising period, rebound in contact, and total free-to-contact sequences after drop/impact energy absorption periods and the drop test event was solved for 0.005 s. A mobile workstation, Dell Precision M4800 Series (Intel Core i7-4910MQ CPU @ 2.90 GHz, NVIDIA Quadro K2100M-2 GB, and Physical Memory Total: 32 GB) was employed as the computing platform. The details of the finite element model and material properties used in the FEA setup are given in Figure 3, Table 3 and Table 4 respectively (ANSYS Product Doc., 2019b; Dumond and Baddour, 2014; Gezer et al., 2012; Matweb LLC, 2020; Puchalski and Brusewitz, 2001).

(**Fig. 3.** Finite element model (a: Reverse engineered apple model, b: Outer mesh structure, c: Inner mesh structure))

(**Table 3.** Details of the finite element model)

(**Table 4.** Material properties)

3. RESULTS

3.1. Weight Loss in Percentage

The weight losses of apples increased during the storage and reached the highest value at the end of the storage period. During cold storage, the maximum (2.87 %) and the minimum (2.35 %) weight losses were recorded in the structural steel-750 mm and control groups, respectively (Supplementary file-2: Table a). Weight loss increased as the storage period was prolonged, regardless of the impact platform and drop height. Additionally, there were no statistical differences between impact surfaces (2.62 %, 2.66 % and 2.68 % HDPE, wood and s. steel, respectively) however, the lowest weight loss was obtained from the control fruit (2.35 %) (Figure 4a).

3.2. Skin Colour: Lightness (L*), Chroma (C*), Hue angle (hº)

The skin colour of apples is one of the most important quality criteria for consumer's purchase. However, when the fruit falls from a height, the colour of the fruit skin turns brown at the point of impact due to bruising. In this study, the lowest lightness (L*) value was found at the steel-750 (49.03) treatment. There were no statistical differences between steel-750 and HDPE-750 cases. The highest L* value (58.37) was at harvest (day 0) and the lowest (48.17) was on day 30 (Supplementary file-2: Table b). There were no statistical differences between control (55.69), HDPE (54.16) and wood (53.39) surfaces. However, fruit damaged from steel (52.23) impact surface lost luminosity more than any other surface (Figure 4b).

Chroma value (C*) values first decreased then increased and reached a peak value (44.74) on day 210 of storage. The highest C* value (43.07) was recorded in the control group and the lowest (38.93) was in the spruce-750 case (Supplementary file-2: Table c). The comparison of the impact surfaces showed that the highest C* value (43.09) was in the control group and the lowest (39.97) was in spruce surface (Figure 4c). It was determined that the drop heights and impact surfaces had no significant effect on the hue value (hº) of apples during storage.

3.3. Ethylene Production and Respiration Rate

Similar to other climacteric fruit, ethylene production is the main reason for ripening and senescence in apples. Additionally, ethylene production is stimulated when plant tissues are bruised and injured (Knee, 2001). In this study, the minimum ethylene production was recorded in the control group (8.37 µL C_2H_4 kg^{-1} h^{-1}) and the maximum production was in the steel-750 (14.41 µL C_2H_4 kg^{-1} h^{-1}) case. Ethylene production first increased and reached a peak value at 120 days of storage (18.27 µL C_2H_4 kg^{-1} h^{-1}) and then decreased during the rest of measurement (Supplementary file-2: Table d). The evaluation made during 10 days of measurement for ethylene production of fruit at 20 ºC (in order to determine the climacteric features of the damaged fruit) showed that ethylene production first increased and reached a peak value at day 4 (14.67 µL C_2H_4 kg^{-1} h^{-1}), then decreased during the rest of measurement. The control fruit reached a peak value at day 6 (11.64 µL C_2H_4 kg^{-1} h^{-1}) and then decreased. The maximum ethylene production was recorded in the HDPE-750 (13.90 µL C_2H_4 kg^{-1} h^{-1}) case and the minimum production was in the control group (8.98 µL C_2H_4 kg^{-1} h^{-1}) (Supplementary file-2: Table e).

The ethylene production of damaged fruit (12.57, 13.17 and 13.41 µL C_2H_4 kg^{-1} h^{-1} wood, HDPE and s. steel, respectively) during storage was determined to be higher than the control fruit (8.37 µL C_2H_4 kg^{-1} h^{-1}). However, no statistical differences were found between steel and HDPE (Figure 4d). At 20 ºC, the ethylene production of the damaged fruit (11.77, 11.91 and 12.35 µL C_2H_4 kg^{-1} h^{-1} wood, s. steel and HDPE, respectively) was higher than the control fruit (8.98 µL C_2H_4 kg^{-1} h^{-1}) and no difference was found between those from different impact surfaces (Figure 4e).

The highest respiration rate was recorded in spruce-750 (0.84 mL CO_2 kg^{-1} h^{-1}) and the lowest was in the control group (0.57 mL CO_2 kg^{-1} h^{-1}). During the storage, the respiration rate of apples fluctuated unlike ethylene production. The highest respiration rate was recorded on day 0 (0.96 mL CO_2 kg^{-1} h^{-1}) and the lowest was on day 30 (0.64 mL CO_2 kg^{-1} h^{-1}) (Supplementary file-2: Table f). At 20 ºC, the highest respiration rate was recorded in wood (spruce)-750 (1.26 mL CO_2 kg^{-1} h^{-1}) and the lowest was in the control group (0.79 mL CO_2 kg^{-1} h^{-1}). However, at 20 ºC, the respiration rate first increased and reached a peak value at day 4 (1.18 mL CO_2 kg^{-1} h^{-1}) then decreased during the rest of measurement (Supplementary file-2: Table g).

The respiration rate of the cold-stored damaged fruit (0.72, 0.76 and 0.81 mL CO_2 kg^{-1} h^{-1} HDPE, s. steel and wood, respectively) was determined to be higher than the control fruit (0.57 mL CO_2 kg^{-1} h^{-1}) (Figure 4f). The respiration rate of the damaged fruit (0.90, 1.12 and 1.18 mL CO_2 kg^{-1} h^{-1} s. steel, HDPE and wood, respectively) was higher than the control fruit (0.79 mL CO_2 kg^{-1} h^{-1}) (Figure 4g). The highest respiration rate was determined to be on those impacting a wood (spruce) surface in both cold storage and 20 ºC. During cold storage, wood was followed by steel and HDPE, respectively, while at 20 ºC, it was recorded as HDPE and steel, respectively (Figure 4f and Figure 4g).

(**Fig. 4.** Experimental results related to physical and chromatographical measurements (means with standard deviations) (a: weight loss, b: lightness value, c: chroma value, d: ethylene production (at 0 °C), e: ethylene production (at 20 °C), f: respiration rate (at 0 °C), g: respiration rate (at 20 °C)) (Impact surfaces of structural steel (S. steel), high-density polyethylene (HDPE) and wood (Spruce), respectively))

3.4. Experimental Results Related to Drop Test

Physical measurements related to the bruising regions of the apple specimens taken at day 0 and during cold storage periods of day 30, day 120 and day 210 were conducted, respectively. The empirical equations were utilised in order to calculate the bruise area and the bruise volume magnitudes of the damaged specimens used in the experimental drop tests. The graphical representations of the physical calculations are given in Figure 5.

(**Fig. 5.** Physical measurements related to bruise area and bruise volume of the tested specimens at day 0 and during periods of storage (means with standard deviations) (a, b and c: Impact surfaces of structural steel, high-density polyethylene (HDPE) and wood (Spruce), respectively))

3.5. FEA Outputs Related to Drop Test

After completion of the FEA processing, the simulation results provided useful visuals and numerical data related to the fruit damage phenomenon. Time dependent stress progression and its distribution on the apple model was clearly exhibited through the simulation visual outputs related to predefined drop events of the fruit (Supplementary file-3). Permanent bruise tracks where the stress regions are beyond the bio-yield stress point of 0.385 MPa on the apple flesh were successfully illustrated. These stress distribution results also allowed measurement of the bruise area and bruise volumes in the digital environment. Additionally, numerical values extracted from the simulation results related to max. equivalent stress, max. contact force, max. internal (absorbed energy) and the energy activity summary, which are very complex to represent through physical experiments, were obtained. A sample simulation visual and graphical representation of the numerical outputs are given in Figure 6 and Figure 7.

(**Fig. 6**. FEA visual outputs and progression plots: Eq. stress, reaction force and internal energy change against time (a: Sample FEA print out, b, c and d: Impact surfaces of structural steel, high-density polyethylene (HDPE) and wood, respectively))

(Fig. 7. FEA outputs: max. equivalent stress (a), max. internal (absorbed energy) (b), max. reaction force (c) and the typical energy activity summary (d) against impact surface and drop height)

3.6. Verification and Validation of the FEA Scenarios

3.6.1. Verification of the Finite Element Model

Finite element model verification which can test the accuracy of the meshed model geometry to represent the digitalised model geometry was made by utilising the skewness metric check in the simulation software. The average skewness metric value of 0.207 was provided on the mesh model. Thus, it provided an accrued verification with an excellent cell quality for the finite element model. Another indicator to be observed in order to test the accuracy of the simulation results is the energy activity summary of the explicit dynamics simulations. In this activity, kinetic energy, internal (absorbed) energy, contact energy and hourglassing/hourglass energy activities should be carefully checked (Figure 7d). Hourglassing is a deformation that produces on volume or strain change in hex/quad meshes in a finite element model. It is essentially a spurious deformation mode of a finite element model, resulting from the excitation of zero-energy degrees of freedom. Therefore, this energy activity is called hourglass energy or zero mode energy which is suggested not to exceed 5-10 % of internal energy in a healthy created FEA (Celik, 2017). In this regard, simulation energy summaries of the FEA scenarios in this study were checked and it was seen that the hourglass energy did not exceed 5-10 % of internal energy values in any of the FEA scenarios. Thus, it was interpreted that the finite element model's element size is appropriate and the accuracy of the FEA is satisfactory under the pre-defined boundary conditions considered in this study.

3.6.2. Validation of the FEA: Comparison of the experimental and FEA data

Experimental and simulation results provided useful information about drop energy activity and bruising geometry of the apple specimens. Firstly, a comparison was made for the total energy calculation, with consideration of the apple mass and drop height, the potential (total) energy affecting the apple specimens at the impact moment were calculated and compared with the simulation results. The comparison extracted a high level of correlation between simulation and analytical calculations: maximum relative differences were 0.414 % at drop heights of 250 mm and 500 mm against minimum relative difference of 0.437 % at drop heights of 750 mm.

As suggested in the literature, bruise area and bruise volume measurements and calculations were conducted respectively, subsequently experimental and simulation results were compared. This validation study revealed that there is a good level of correlation between the experimental and FEA results on the bruise area. Maximum relative difference was 8.475 % at the drop height of 500 mm (impact surface: wood) against minimum relative difference of 1.919 % at the drop height of 750 mm (impact surface: wood). The average value of the relative differences for all bruise area comparisons was 5.501 %. However, opposite to this good level of correlation between bruise area values (experimental and FEA), experimental bruise volume measurements and FEA results did not provide a good level of correlation. The simulation study revealed higher bruise volume values, which is the maximum relative difference: 288.4 % at drop height of 250 mm (impact surface: HDPE); minimum relative difference was119.94 % at the drop height of 500 mm (impact surface: Wood). The average value of the relative differences for all bruise volume comparisons was 183.12 %. Graphical representation of the comparisons made for the validation study are given in Figure 8.

(**Fig. 8.** Graphical representation of the comparisons made for the validation study (a: Total Energy Comparison, b, c and d: Impact surfaces of structural steel, high-density polyethylene (HDPE) and wood, respectively))

3.6.3. Bruise Susceptibility

The validation study revealed a good interaction between experimental and FEA results for bruise area comparisons after drop damage occurred on the fruit (Day-0). This result indicated that utilising the bruise area instead of bruise volume is a better measure in calculation / expression of the bruise susceptibility. The calculations related to the bruise susceptibility (based on FEA bruise area measurements) at certain thresholds (at material yield stress point: the permeant deformation threshold) and at the rebounding point, were graphically represented in Figure 9.

(**Fig. 9.** Bruise susceptibility calculations (FEA) (a: Bruise area based bruise susceptibility thresholds (at material yield stress point), b: Bruise area based bruise susceptibility calculations (after rebound point), c: Ethylene production after drop case))

4. DISCUSSION

The analysis results revealed that the weight loss increased during the storage period regardless of the impact surface and drop height. Furthermore, damaged fruit lost more weight compared to the control group. Mechanical injury often damages the barriers to water loss and can thus increase the rate of water loss from the fruit. The increase in respiration rate due to injury may lead to higher levels of weight loss in damaged fruit (Bryant, 2004). Furthermore, the bruised area in the fruit positively correlated with the higher weight loss (Xia et al., 2020). The increase in weight loss in apples may be due to an increase in ethylene production and respiration rate. Additionally, ethylene production and respiration rate measurements in this study verified the argument. The outcomes discussed here agreed with (Wei et al., 2019) and (Santos et al., 2004). They reported that an increase in weight loss with prolonged storage time and damaged fruit suffered with higher weight loss in kiwi and mango fruit. In another study, (Hussein et al., 2019) reported that higher weight loss occurred when the drop height increased in pomegranate fruit, similar to this study.

Additionally, the study revealed that the damaged surfaces of the fruit darkened (decreased L*) and increased the colour intensity (increased C*) on the fruit skin. It was also observed that the skin turned brown in the damaged parts of the fruit. This can be because of phenolic compounds in apple cell vacuoles, brought in contact with catechol oxidase in the plastids resulting from the mechanical damage, leading to the formation of quinones polymerizing to a dark colour (Van Zeebroeck et al., 2007). In 'Granny Smith' apples at 96 hours, bruise damage caused the decreased L* value and increased C* value (Samim and Banks, 1993), which are outcomes that are in agreement with the study reported here.

Apple is a climacteric fruit that is responsive to ethylene and undergoes a significant increase in respiration and ethylene production during ripening (Yang et al., 2013). When apples are damaged, ethylene production and respiration rate increase (Lu et al., 2019). This increase is greatly affected by the extent of mechanical damage on the fruit (Mencarelli et al., 1996). In this study, ethylene production increased with the mechanical damage. Similar to the outcomes reported here, a study in 'Gala' apples showed that mechanical injury caused the ethylene production. Conversely, there was no relation between mechanical injury and respiration rate (Steffens et al., 2008). Furthermore, the oxidation of phenolic compounds by catechol oxidase causes a transient increase in oxygen uptake by the damaged tissue, but there are more lasting effects on the cellular respiration of adjacent, undamaged tissue (Knee, 2001). (Hussein et al., 2019) reported that respiration rate increased with higher bruise damage and storage temperature. Also, after damage, if the fruit is kept at a warmer temperature, the bruise penetrates deeper and colder temperatures decrease bruising damage (Cui et al., 2018). In this study, respiration rate of the fruit at 20 ºC was higher than cold stored fruit. Generally, it is thought that the rapidly increasing respiration rate with damage decreases with the functioning of cell repair mechanisms or due to the decrease in temperature after the fruit are placed in storage (Li and Thomas, 2014).

Experimental results related to physical bruising revealed the progression of the bruise area and bruise volume during storage time related to impact surface and drop height (Figure 7). In these charts, it was seen that there is a clear increase in both bruise area and bruise volume against storage period: the highest bruising progression was seen at day 210 regardless of the impact surface and the drop height. This indicated that the bruising increase has a direct relationship with storage period.

Simulation results (Figure 8 and Figure 9) indicated that the maximum equivalent stress value was 0.606 MPa on the HDPE impact surface with an impact height of 750 mm. The minimum equivalent stress value of 0.511 MPa was calculated at the impact surface of wood (spruce) and impact height of 250 mm. These sequences were very similar for internal energy absorption magnitudes. The results also clearly exhibited that the highest values of maximum stress, reaction force and internal energy absorption magnitudes were observed at the highest drop height of 750 mm. In addition to this, although there are clear differences for these values against drop heights, the effect of the impact surface on the stresses, reaction force and internal energy magnitudes was not magnificent.

Bruise susceptibility threshold for the apple variety value was appointed according to the material yield stress point (permeant deformation threshold). The susceptibility calculation at this point indicated very logical results which is an increase in the susceptibility against the drop heights. At this point, an approximate linear increase was seen on the bruise area measurements against drop heights, however because of the rapid deformation phenomena of the impact during the drop test, internal energy values were seen to decrease (Figure 9a). The highest susceptibility was calculated on impact surfaces of steel, wood and HDPE at drop heights of 250 mm, 500 mm and 750 mm respectively. This occurrence was coherent with ethylene production just after the drop damage phenomenon of the apple specimens (Figure 9c). This can also be considered as proof of the accurate damage phenomenon simulated in this study. However, the bruise susceptibility values at the end of the first rebound after the drop impact considered in this study were calculated by considering maximum values of FEA numerical outputs such as maximum values of the bruise area and the internal energy. For these calculations, decreases were observed on the bruise susceptibility values against drop heights of 250 mm, 500 mm and 750 mm respectively. The reason for this progression can be explained with bi-linear elastoplastic material model assigned in the FEA scenarios. After the first yield stress point (0.385 MPa), the material experienced permanent deformation and continued to second sequence of elastic behaviour at the plastic deformation region. This was a more realistic deformation description against previous FEA studies considering linear material models. Therefore, bruises area values were not a linear increase against maximum internal energy values at 250 mm, 500 mm and 750 mm respectively (Figure 9b).

Additionally, it is a well-known issue; FEA is a numerical analysis technique that can provide approximate solutions (that require physical or experimental verification), therefore errors in a FEA can occur. These are mostly methodical and numerical errors and they may result during the establishment of the mathematical model (e1), the mathematical discontinuity (e2) and the numerical solution processes (e3) (Narasaiah, 2008; Pancoast, 2009; Salmi, 2008). In this regard, in order to evaluate the accuracy level of the simulation results, verification and validation studies should be carried out. In this study, the FEA model and the results were verified by means of a skewness metric check and hourglass energy evaluation respectively. High level verification was provided. The validation study showed that there is a good union when comparing the bruise area measurements between experimental and FEA measurements however, comparison on bruise volume measurements did not provide such a correlation. The reason for these high-level differences can be explained from the modelling strategy and empirical approach in experimental measurements. The model used in these FEA simulations did not consider the core, seed and skin components of the apple. It can be interpreted that most especially, the skin has an important role for the internal stress progression and might be preventing the stress progression in the direction to the centre of the apple geometry. Another contribution to this high-level difference might be made by the empirical calculations as the errors are unavoidable during physical measurements and because of the mathematical assumptions in these empirical expressions. Additionally, this study indicated an agreement with (Pang et al., 1996)'s report: bruise surface was a better parameter for assessing damage than the bruise volume, most especially from simulation studies which are focusing on flesh bruising.

Although, some studies in the literature indicate that relative difference may vary up to 30 % depending on the complexity of the physical environment to be simulated against the physical environment, there is a belief that a relative difference rate of 10 % (approx.) should be provided between FEA and experimental validation studies (Krutz et al., 1984; Sakakibara, 2008). Besides this, it is a well-known issue that the scale of the absolute numerical results should also be kept under consideration and differences between experimental and simulation-based results can vary dependent on set-up conditions and assumptions made in the FEA and the unpredictable physical environment conditions during the experiments. As shown in this study, absolute values of the stress magnitude are relatively small and these types of relatively small absolute numerical values may lead to high percentage differences between experimental and FEA results. Therefore, the factors mentioned above should be taken into consideration in the comparative evaluation of the experimental and FEA results. Finally, in can be concluded that the FEA of a bruising phenomenon under impact loading of the drop test of the 'Pink Lady' apple was successfully exemplified.

5. CONCLUSION

During long-term cold storage periods of the damaged apples, the loss of volumetric weight, surfaces lightness and chroma values was significantly clear. Ethylene production and respiration rates rapidly increased just after the fruit damage and continued to increase during the storage periods. Additionally, deformation/stress/damage progression in time during impact loading was clearly exhibited through a realistic simulation set up strategy. Ethylene production was coherent with calculated bruise susceptibility regarding the data extracted from the simulation outputs. Verification and validation procedures for the simulation were also achieved with high accuracy results in the study. In focus, the specific bruising area based bruise susceptibility thresholds for a specific product (the 'Pink Lady' apple) were presented against different impact materials and drop heights. This is very important data for the postharvest processing and packaging industry. It is advisable that utilising elastoplastic material models in the FEA studies related to the deformation analysis of agricultural products should be focused on for more realistic simulation results. The drop test revealed permanent damage progression regarding the impact surfaces of steel, HDPE and wood materials, however, the study results may advise others to consider the impact platform materials which have lower elastic modulus properties such as paper cardboard, rubber etc. in future studies in order to observe fruit-softer material impact phenomenon. Based on the experimental validation study, another critical extraction from this study is, most especially for FEA-based simulation studies focused on product flesh deformation (ignoring components such as skin, core etc.), that the bruising area measurement is more accurate than bruise volume measurement when evaluating bruising of similar solid-like agricultural products.

Acknowledgement

This research was supported financially by The Scientific Research Projects Coordination Unit of Akdeniz University (Antalya, Turkey). The authors declare that they have no known competing financial interests or personal relationships that could have appeared to influence the work reported in this paper.

REFERENCES

Abedi, G., Ahmadi, E., 2013. Design and evaluation a pendulum device to study postharvest mechanical damage in fruit: Bruise modeling of red delicious apple. Aust. J. Crop Sci. 7, 962–968.

ANSYS Product Doc., 2019a. ANSYS Meshing User’s Guide: Skewness (Release 2019 R2). ANSYS Inc., USA.

ANSYS Product Doc., 2019b. ANSYS Engineering Data User’s Guide: Basics of Engineering Data (Release 2019 R2). ANSYS Inc., USA.

ASABE Standard, 2017. ASAE S368.4 DEC2000 (R2017) - Compression Test of Food Materials of Convex Shape [WWW Document]. Am. Soc. Agric. Biol. Eng.

Bollen, A.F., Nguyen, H.X., Dela Rue, B.T., 1999. Comparison of methods for estimating the bruise volume of apples. J. Agric. Eng. Res. 74, 325–330. https://doi.org/10.1006/jaer.1999.0468

Brusewitz, G.H., Bartsch, J.A., 1989. Impact parameters related to post harvest bruising of apples. Trans. Am. Soc. Agric. Eng. 32, 953–957. https://doi.org/10.13031/2013.31097

Bryant, P., 2004. Optimising the Postharvest Management Of Lychee (Litchi chinensis Sonn.)-A Study of Mechanical Injury and Desiccation. University of Sydney. Crop Science.

Cardenas-Weber, M., Stroshine, R.L., Haghighi, K., Edan, Y., 1991. Melon material properties and finite element analysis of melon compression with application to robot gripping. Trans. Am. Soc. Agric. Eng. 34, 920–929. https://doi.org/10.13031/2013.31750

Celik, H.K., 2017. Determination of bruise susceptibility of pears (Ankara variety) to impact load by means of FEM-based explicit dynamics simulation. Postharvest Biol. Technol. 128, 83–97. https://doi.org/10.1016/j.postharvbio.2017.01.015

Celik, H.K., Rennie, A.E.W., Akinci, I., 2011. Deformation behaviour simulation of an apple under drop case by finite element method. J. Food Eng. 104, 293–298. https://doi.org/10.1016/j.jfoodeng.2010.12.020

Cui, J., Yang, M., Son, D., Park, S., Cho, S.I., 2018. Estimation of tomato bruising by mechanical impact force using multivariate analysis. HortScience 53, 1352–1359. https://doi.org/10.21273/HORTSCI13066-18

Dumond, P., Baddour, N., 2014. Mechanical Property Relationships in Sitka Spruce Soundboard Wood, in: International Conference on Noise and Vibration Engineering, ISMA 2014. International Conference on Noise and Vibration Engineering, ISMA 2014, Le Mans, pp. 287–293.

Eissa, A.H.A., Alghannam, A.R.O., Azam, M.M., 2012. Mathematical Evaluation Changes in Rheological and Mechanical Properties of Pears during Storage under Variable Conditions. J. Food Sci. Eng. 2. https://doi.org/10.17265/2159-5828/2012.10.004

Fadiji, T., Coetzee, C., Chen, L., Chukwu, O., Opara, U.L., 2016. Susceptibility of apples to bruising inside ventilated corrugated paperboard packages during simulated transport damage. Postharvest Biol. Technol. 118, 111–119. https://doi.org/10.1016/j.postharvbio.2016.04.001

FAOSTAT, 2019. Food and Agriculture Organization of the United Nations [WWW Document]. Food Agric. Organ. United Nations. URL http://www.fao.org (accessed 4.4.21).

Garcia, C., Ruiz-Altisent, M., Chen, P., 1988. Impact parameters related to bruising in selected fruit, in: ASAE, (American Society of Agricultural Engineers Meeting) (ASAE Paper No. 88-6027.). p. 16.

Gezer, İ., Musa Özcan, M., Hacıseferoğulları, H., Çalışır, S., 2012. International Journal of Farming and Allied Sciences Some nutritional and physical properties of crab apple (Malus silvestris Mill.) fruit. Int. J. Farming Allied Sci. 1, 101–107.

Holt, J.E., Schoorl, D., 1977. Bruising and Energy Dissipation in Apples. J. Texture Stud. 7, 421–432. https://doi.org/10.1111/j.1745-4603.1977.tb01149.x

Hussein, Z., Fawole, O.A., Opara, U.L., 2019. Bruise damage susceptibility of pomegranates (Punica granatum, L.) and impact on fruit physiological response during short term storage. Sci. Hortic. (Amsterdam). 246, 664–674. https://doi.org/10.1016/j.scienta.2018.11.026

Kabas, O., Celik, H.K., Ozmerzi, A., Akinci, I., 2008. Drop test simulation of a sample tomato with finite element method. J. Sci. Food Agric. 88, 1537–1541. https://doi.org/10.1002/jsfa.3246

Knee, M., 2001. Fruit Quality and its Biological Basis (Sheffield Biological Siences), 1st ed. Blackwell.

Komarnicki, P., Stopa, R., Szyjewicz, D., Młotek, M., 2016. Evaluation of bruise resistance of pears to impact load. Postharvest Biol. Technol. 114, 36–44. https://doi.org/10.1016/j.postharvbio.2015.11.017

Krutz, G., Thompson, L., Claar, P., 1984. Design of agricultural machinery., Design of agricultural machinery. John Wiley and Sons, New York.

Lewis, R., Yoxall, A., Marshall, M.B., Canty, L.A., 2008. Characterising pressure and bruising in apple fruit. Wear 264, 37–46. https://doi.org/10.1016/j.wear.2007.01.038

Li, Z., Thomas, C., 2014. Quantitative evaluation of mechanical damage to fresh fruit. Trends Food Sci. Technol. https://doi.org/10.1016/j.tifs.2013.12.001

Lu, F., Xu, F., Li, Z., Liu, Y., Wang, J., Zhang, L., 2019. Effect of vibration on storage quality and ethylene biosynthesis-related enzyme genes expression in harvested apple fruit. Sci. Hortic. (Amsterdam). 249, 1–6. https://doi.org/10.1016/j.scienta.2019.01.031

Lu, Y., Lu, R., 2017. Non-destructive defect detection of apples by spectroscopic and imaging technologies: A review. Trans. ASABE. https://doi.org/10.13031/trans.12431

Matweb LLC, 2020. Online Materials Information Resource [WWW Document]. http://www.matweb.com. URL http://www.matweb.com/ (accessed 10.3.20).

Mditshwa, A., Fawole, O.A., Opara, U.L., 2018. Recent developments on dynamic controlled atmosphere storage of apples—A review. Food Packag. Shelf Life. https://doi.org/10.1016/j.fpsl.2018.01.011

Mencarelli, F., Massantini, R., Botondi, R., 1996. Influence of impact surface and temperature on the ripening response of kiwifruit. Postharvest Biol. Technol. 8, 165–177. https://doi.org/10.1016/0925-5214(95)00070-4

Mohsenin, N.N., 1986. Physical properties of plant and animal materials, 2nd ed, Gordon and Breach Science Publishers. Gordon and Breach Science Publishers, New York.

Musacchi, S., Serra, S., 2018. Apple fruit quality: Overview on pre-harvest factors. Sci. Hortic. (Amsterdam). https://doi.org/10.1016/j.scienta.2017.12.057

Narasaiah, G.L., 2008. Finite Element Analysis. B.S. Publications.

Opara, U.L., Pathare, P.B., 2014. Bruise damage measurement and analysis of fresh horticultural produce-A review. Postharvest Biol. Technol. 91, 9–24. https://doi.org/10.1016/j.postharvbio.2013.12.009

Pancoast, D., 2009. Solidworks Simulation-2010 Training Manual, PMT1040-EN ed. Dassault System - Solidworks Corporation.

Pang, D.W., Studman, C.J., Banks, N.H., Baas, P.H., 1996. Rapid assessment of the susceptibility of apples to bruising. J. Agric. Eng. Res. 64, 37–47. https://doi.org/10.1006/jaer.1996.0044

Puchalski, C., Brusewitz, G.H., 2001. Fruit ripeness and temperature affect friction coefficient of McLemore and Gala apples. Int. Agrophysics 15, 109–114.

Sakakibara, N., 2008. Finite Element in Fracture Mechanics (Lecture Notes: The University of Texas).

Salmi, S., 2008. Multidisciplinary Design Optimization in an Integrated CAD / FEM Environment 81.

Samim, W., Banks, N.H., 1993. Color Changes in Apple Bruises Over Time. Acta Hortic. 304–306. https://doi.org/10.17660/actahortic.1993.343.73

Santos, E.C., Silva, S.M., Santos, A.F., Mendonça, R.M.N., Silveira, I.R.B.S., Lira, M.L.S., Silva, L.R., Alves, R.E., 2004. Influence of 1-Methylcyclopropene on Ripening and Conservation of Tree-Dropped Mango Fruit Cv. Rosa. Acta Hortic. 573–579. https://doi.org/10.17660/actahortic.2004.645.75

Sitkei, G., 1987. Mechanics of Agricultural Materials. Elsevier 487.

Steffens, C.A., Espíndola, B.P., Do Amarante, C.V.T., Silveira, J.P.G., Chechi, R., Brackmann, A., 2008. Respiração, produção de etileno e qualidade de maçãs “Gala” em função do dano mecânico por impacto e da aplicação de 1-metilciclopropeno. Cienc. Rural 38, 1864–1870. https://doi.org/10.1590/S0103-84782008000700010

Van Zeebroeck, M., Van linden, V., Ramon, H., De Baerdemaeker, J., Nicolaï, B.M., Tijskens, E., 2007. Impact damage of apples during transport and handling. Postharvest Biol. Technol. https://doi.org/10.1016/j.postharvbio.2007.01.015

Wei, X., Xie, D., Mao, L., Xu, C., Luo, Z., Xia, M., Zhao, X., Han, X., Lu, W., 2019. Excess water loss induced by simulated transport vibration in postharvest kiwifruit. Sci. Hortic. (Amsterdam). 250, 113–120. https://doi.org/10.1016/j.scienta.2019.02.009

Xia, M., Zhao, X., Wei, Xiaopeng, Guan, W., Wei, Xiaobo, Xu, C., Mao, L., 2020. Impact of packaging materials on bruise damage in kiwifruit during free drop test. Acta Physiol. Plant. 42, 119. https://doi.org/10.1007/s11738-020-03081-5

Yang, X., Song, J., Campbell-Palmer, L., Fillmore, S., Zhang, Z., 2013. Effect of ethylene and 1-MCP on expression of genes involved in ethylene biosynthesis and perception during ripening of apple fruit. Postharvest Biol. Technol. 78, 55–66. https://doi.org/10.1016/j.postharvbio.2012.11.012

TABLE CAPTIONS

Table 1. Dimensional features of the apple

Table 2. List of the abbreviations used in the equations and related dimensions

Table 3. Details of the finite element model

Table 4. Material properties

FIGURE CAPTIONS

Fig. 1. Application algorithm for bruising and quality investigation of apple 'Pink Lady'

Fig. 2. The portable drop test apparatus, testing scenario (a) and the dimensions used in bruising assessment (b).

Fig. 3. Finite element model (a: Reverse engineered apple model, b: Outer mesh structure, c: Inner mesh structure)

Fig. 4. Experimental results related to physical and chromatographical measurements (means with standard deviations) (a: weight loss, b: lightness value, c: chroma value, d: ethylene production (at 0 °C), e: ethylene production (at 20 °C), f: respiration rate (at 0 °C), g: respiration rate (at 20 °C)) (Impact surfaces of structural steel (S. steel), high-density polyethylene (HDPE) and wood (Spruce), respectively)

Fig. 5. Physical measurements related to bruise area and bruise volume of the tested specimens at day 0 and during periods of storage (means with standard deviations) (a, b and c: Impact surfaces of structural steel, high-density polyethylene (HDPE) and wood (Spruce), respectively)

Fig. 6. FEA visual outputs and progression plots: Eq. stress, reaction force and internal energy change against time (a: Sample FEA print out, b, c and d: Impact surfaces of structural steel, high-density polyethylene (HDPE) and wood, respectively)

Fig. 7. FEA outputs: max. equivalent stress (a), max. internal (absorbed energy) (b), max. reaction force (c) and the typical energy activity summary (d) against impact surface and drop height

Fig. 8. Graphical representation of the comparisons made for the validation study (a: Total Energy Comparison, b, c and d: Impact surfaces of structural steel, high-density polyethylene (HDPE) and wood, respectively)

Fig. 9. Bruise susceptibility calculations (FEA) (a: Bruise area based bruise susceptibility thresholds (at material yield stress point), b: Bruise area based bruise susceptibility calculations (after rebound point), c: Ethylene production after drop case)

Table 1. List of the abbreviations used in the equations and related dimensions

Parameter	Unit	Parameter	Unit	Parameter	Unit
m : Apple mass	(kg)	h_a : Apple height	(mm)	A_b : Bruise area	(mm^2)
h_d : Drop height	(m)	d_a : Apple diameter (average)	(mm)	V_b : Bruise volume	(mm^3)
h_r : Rebound height	(m)	d_b : Bruise depth	(mm)	S_{bV} : Bruise susceptibility (Volume)	($mm^3 \cdot J^{-1}$)
g : Earth gravity	($9.81\ m \cdot s^{-2}$)	W_{b1} : Bruise width (horizontal)	(mm)	S_{bA} : Bruise susceptibility (Area)	($mm^2 \cdot J^{-1}$)
		W_{b2} : Bruise width (vertical)	(mm)	E_i : Total energy at impact	(Joule)
				E_A : Absorbed impact (internal) energy	(Joule)

Table 2. Dimensional features of the apple

Dimensions and calculations		**Unit**	**CAD model measurement**
	Length (z)		64.330
Volumetric dimensions	Height (y)*	(mm)	68.320
	Width (x)*		68.320
Mass**		(kg)	0.142
Volume***		(mm^3)	165642.620
Surface area***		(mm^2)	15162.140
Sphericity	$[(x.y.z)^{1/3}) / z]$	(-)	0.980

** Average diameter*
*** Whole apple mass was calculated automatically through cylindrical specimen density (855.550 kg m^{-3}).*
**** Whole apple volume and surface area values were calculated automatically in solid modelling software.*

Table 3. Details of the finite element model

Meshing		**Element details**		
Meshing strategy	: Curvature based and local sizing	Element size (mm)	(Max.)	: 10
			(Min.)	: 0.05
		Total elements		: 171097
Element type(s)	: Tet4 & Hex8	Total nodes		: 41102
Cell quality	: 0.207*			

** Average skewness value: Excellent (ANSYS product doc., 2019)*

Table 4. Material properties

	Materials	Orientation	Modulus of elasticity ($tan\alpha$) (MPa)	Tangent modulus ($tan\beta$) (Curve-01) (MPa)	Poisson's ratio (-)	Bioyield/Yield stress point (MPa)	Ultimate stress point (MPa)	Force at Bioyield/Yield stress point (N)	Density (Average) (kg m^{-3})	Static coefficient of friction (Apple to impact surface) (-)	Dynamic coefficient of friction (Apple to impact surface) (-)
Fruit *(Apple-Pink Lady)*	Flesh (mesocarp) (Test specimen: Ø 20 mm x 25 mm)	Transverse	4.175 [1] *(R^2: 1)*	1.738 [2] *(R^2: 0.983)*	0.27 ± 0.02 [C]	0.385 ± 0.04 [C]	0.555 ± 0.07 [C]	68.133 ± 7.50 [C]	855.550 ± 43.83 [3]	-	-
Impact surface material	Structural steel	Isotropic	200000 [5]	-	0.30 [4]	250 [4, T]	460 [4, T]	-	7850	0.324 [6]	0.281 [6]
	Plastic-HDPE (Polyethylene - high density)	Isotropic	1100 [4]	-	0.42 [4]	25 [4, T]	33 [4, T]	-	952	0.28 [7]	0.25 [7]
	Wood (spruce)	Isotropic	12571 [5]	-	0.394 [5]	25 [5, C]	84 [5, T]	-	404	0.329 [6]	0.298 [6]

1. Modulus of elasticity (tan α): Slope of the average true stress-true strain curve in elastic region (experimental)
2. Tangent modulus (tan β): Slope of the average true stress-true strain curve-01 in plastic region (experimental)
3. Density value is experimental data
4. ANSYS product material library (ANSYS Product Doc., 2019)
5. Dumond and Baddour, 2014 & WebMat, 2019 (www.matweb.com)
6. Gezer et al, 2012
7. Puchalski and Brusewitz, 2001
T: Tensile properties
C: Compression properties

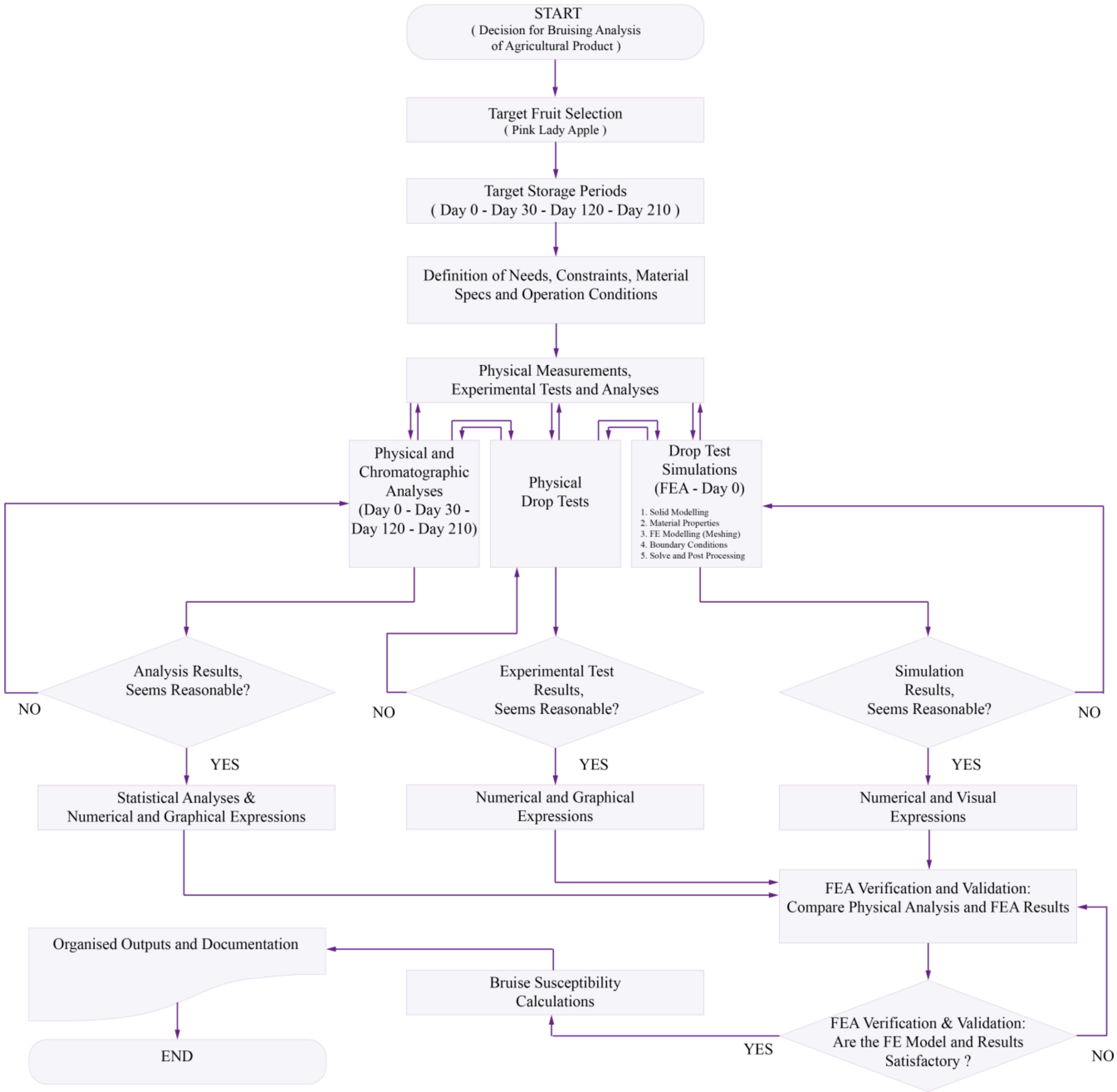

Fig. 1. Application algorithm for bruising and quality investigation of apple ‘Pink Lady’

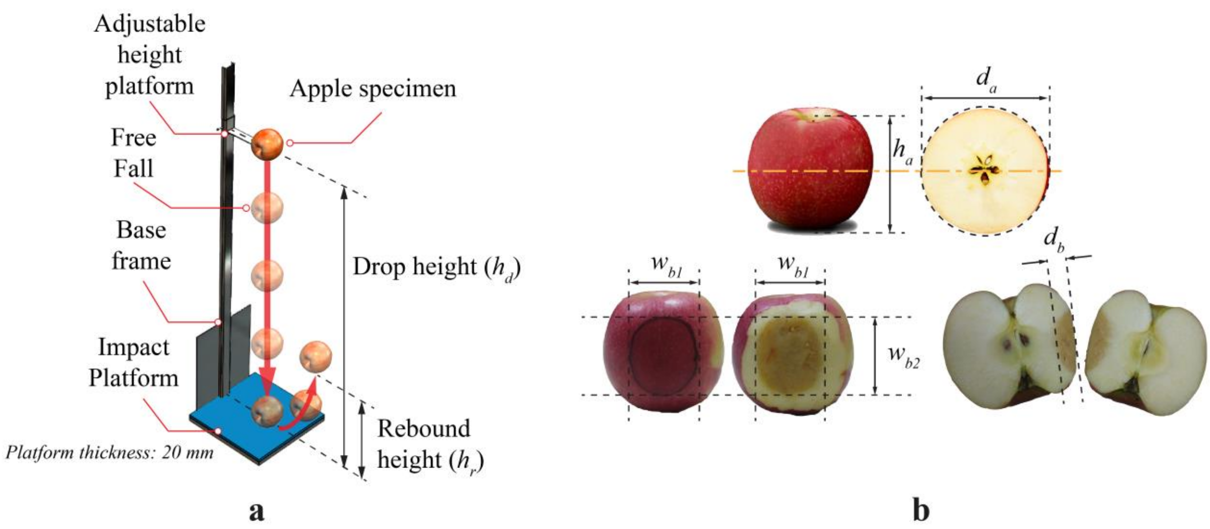

Fig. 2. The portable drop test apparatus, testing scenario (a) and the dimensions used in bruising assessment (b).

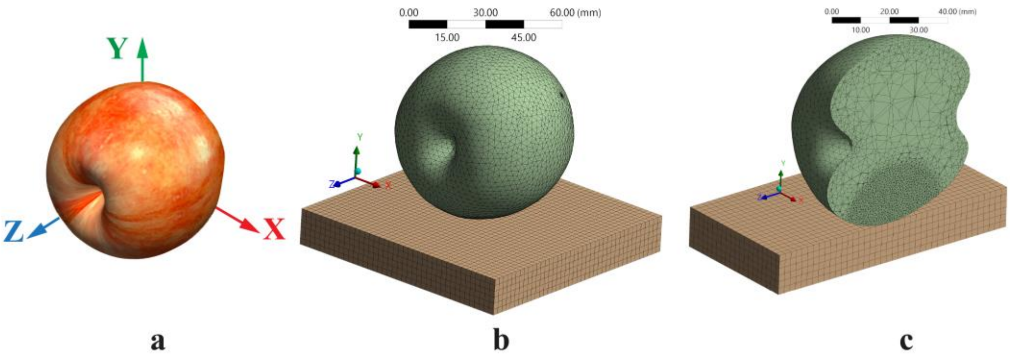

Fig. 3. Finite element model (a: Reverse engineered apple model, b: Outer mesh structure, c: Inner mesh structure)

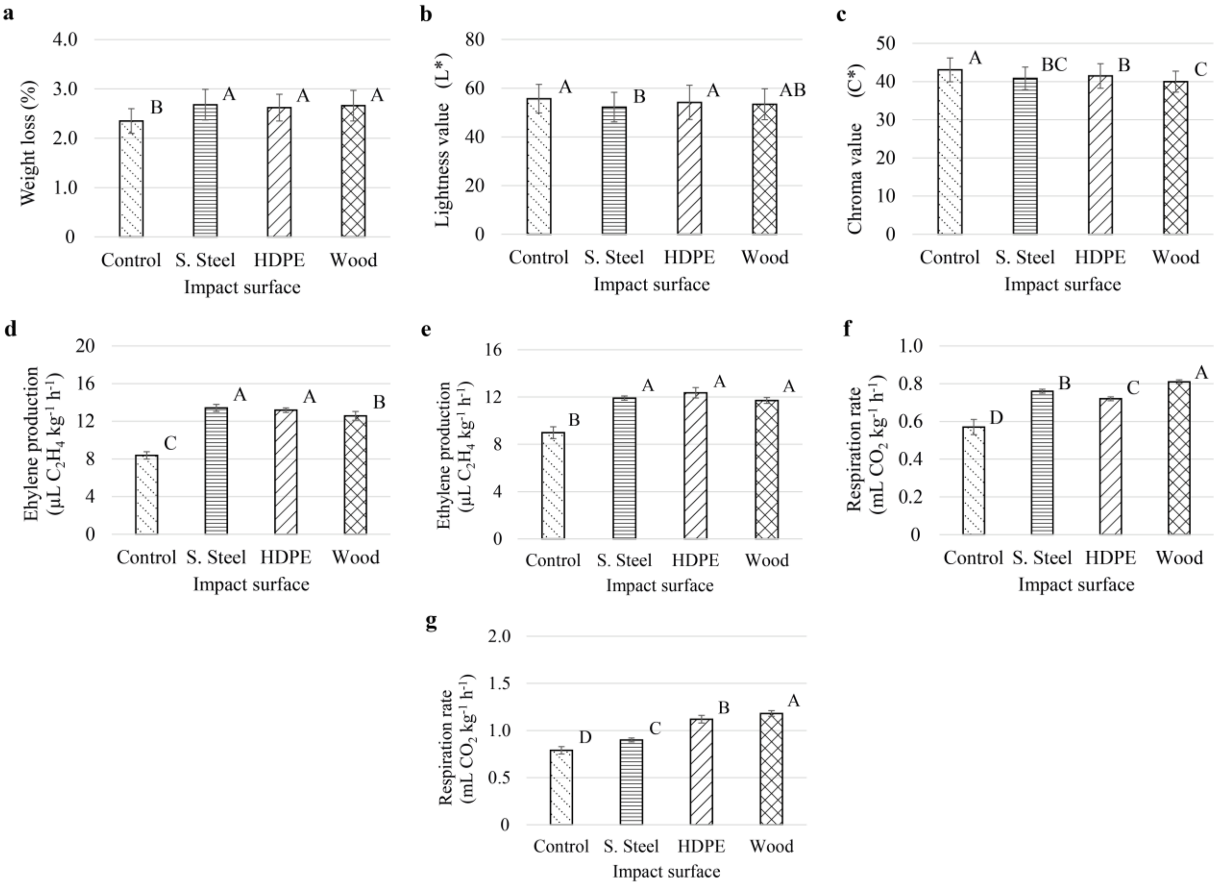

Fig. 4. Experimental results related to physical and chromatographical measurements (means with standard deviations) (a: weight loss, b: lightness value, c: chroma value, d: ethylene production (at 0 °C), e: ethylene production (at 20 °C), f: respiration rate (at 0 °C), g: respiration rate (at 20 °C)) (Impact surfaces of structural steel (S. steel), high-density polyethylene (HDPE) and wood (Spruce), respectively)

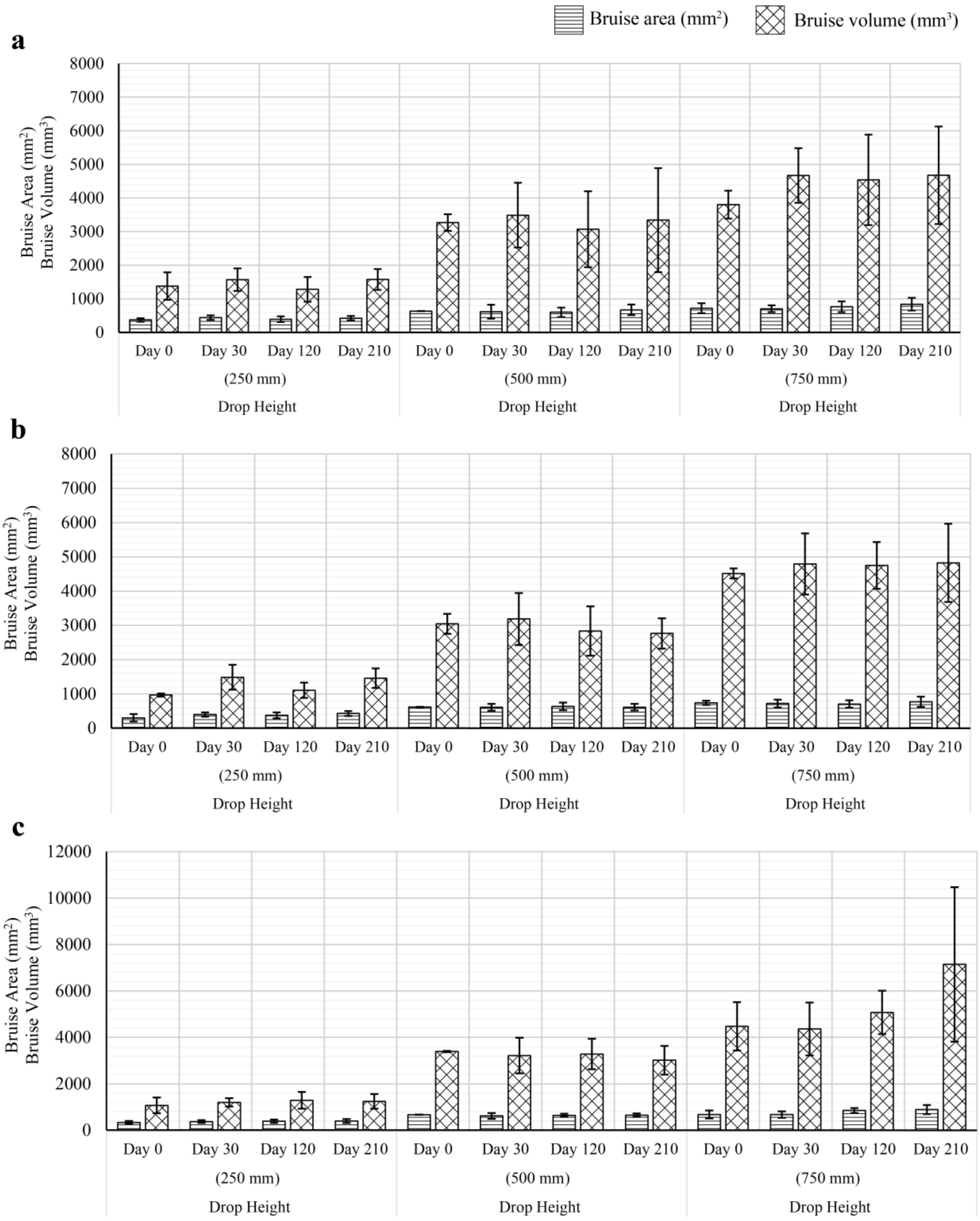

Fig. 5. Physical measurements related to bruise area and bruise volume of the tested specimens at day 0 and during periods of storage (means with standard deviations) (a, b and c: Impact surfaces of structural steel, high-density polyethylene (HDPE) and wood (Spruce), respectively)

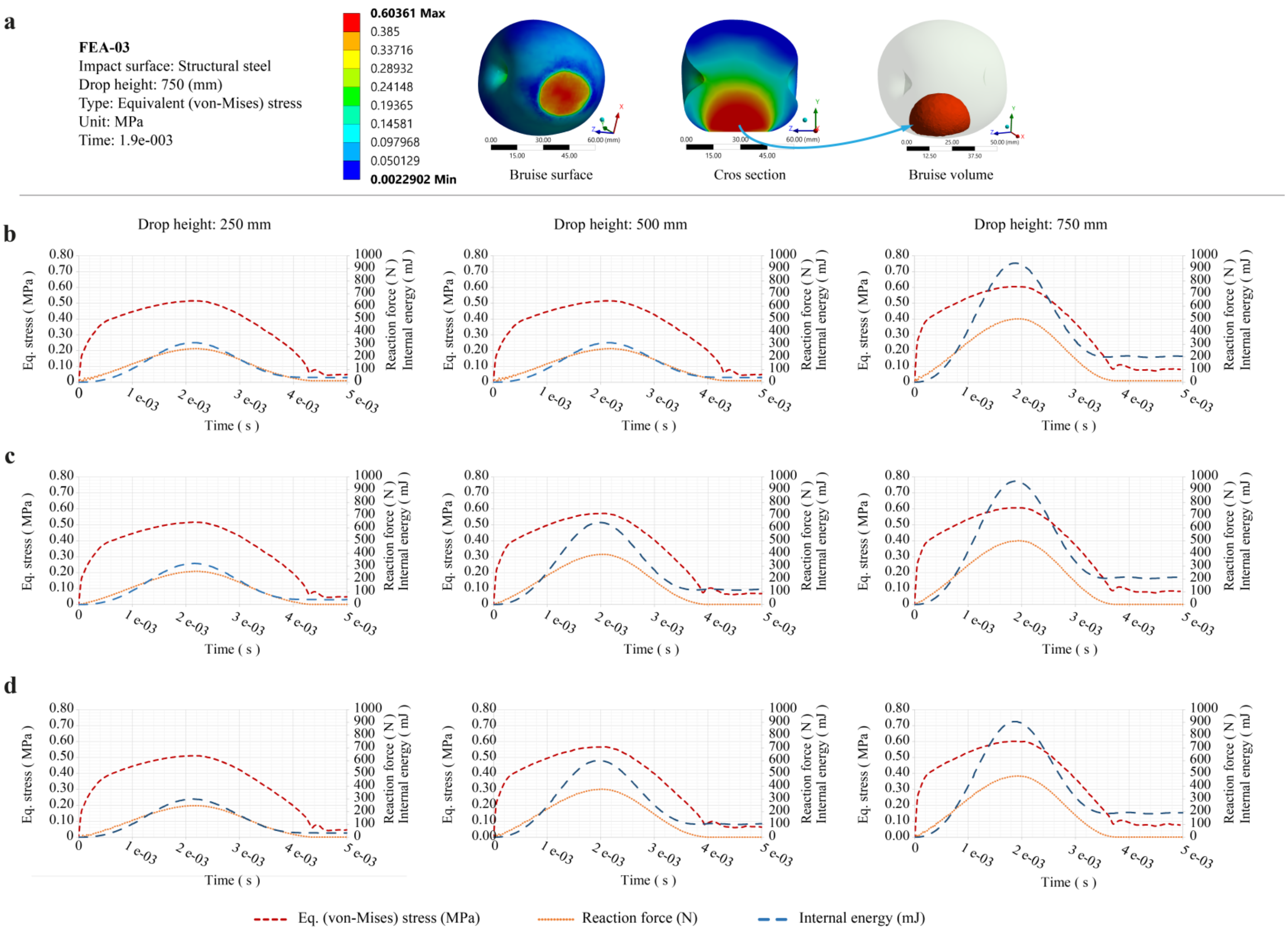

Fig. 6. FEA visual outputs and progression plots: Eq. stress, reaction force and internal energy change against time (a: Sample FEA print out, b, c and d: Impact surfaces of structural steel, high-density polyethylene (HDPE) and wood, respectively)

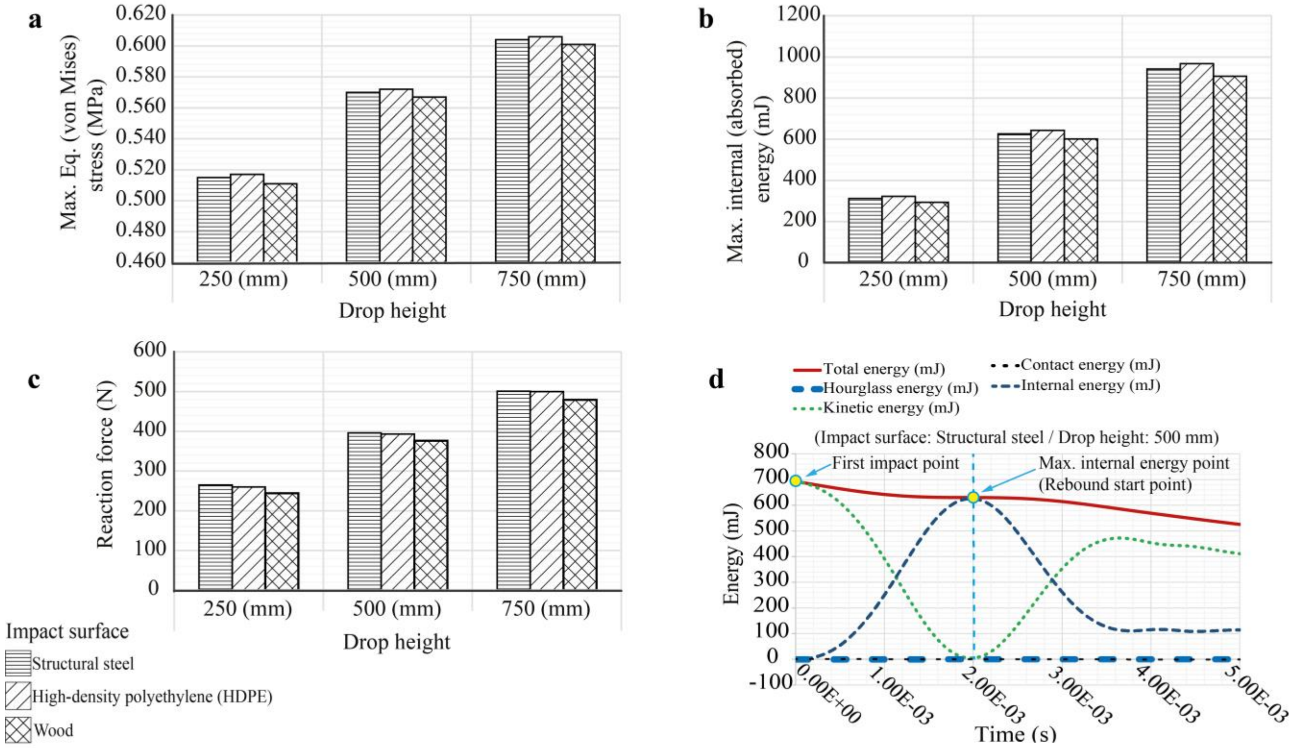

Fig. 7. FEA outputs: max. equivalent stress (a), max. internal (absorbed energy) (b), max. reaction force (c) and the typical energy activity summary (d) against impact surface and drop height

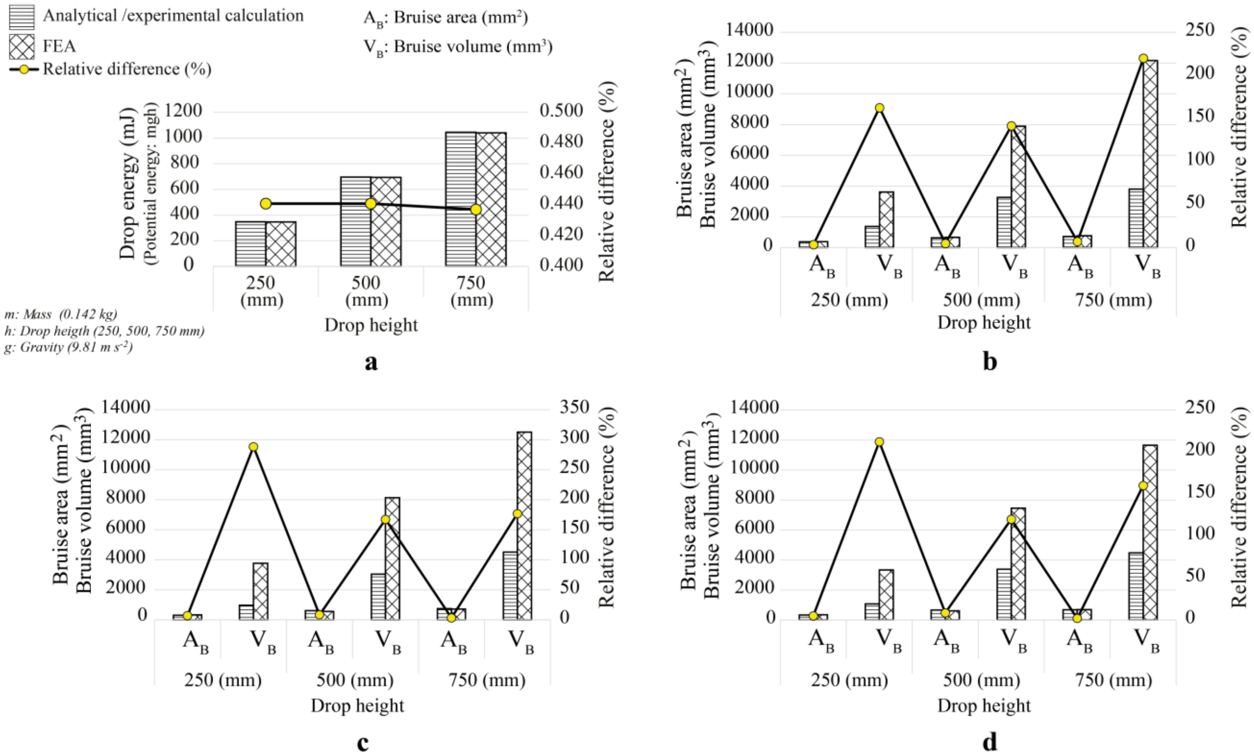

Fig. 8. Graphical representation of the comparisons made for the validation study (a: Total Energy Comparison, b, c and d: Impact surfaces of structural steel, high-density polyethylene (HDPE) and wood, respectively)

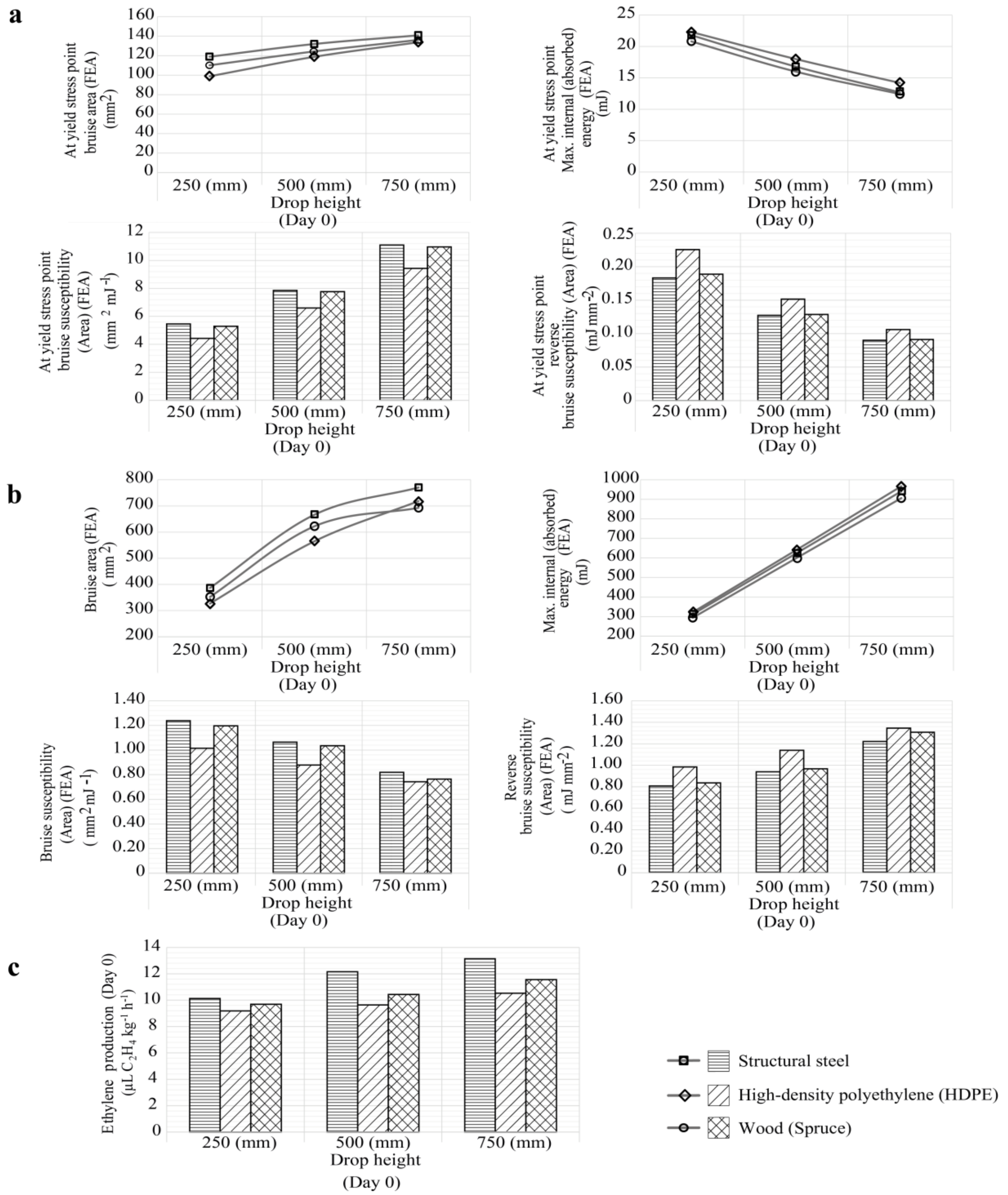

Fig. 9. Bruise susceptibility calculations (FEA) (a: Bruise area based bruise susceptibility thresholds (at material yield stress point), b: Bruise area based bruise susceptibility calculations (after rebound point), c: Ethylene production after drop case)